doi:10.15625/2525-2518/18511



# Effect of rice husk morphology on the ability to synthesize silicon carbide by pyrolysis method

Kieu Do Trung Kien<sup>1, 2, \*</sup>, Ong Dieu Hanh<sup>1, 2</sup>, Nguyen Hoang Thien Khoi<sup>1, 2</sup>, Huynh Ngoc Minh<sup>1</sup>

<sup>1</sup>Faculty of Materials Technology, Ho Chi Minh City University of Technology (HCMUT), 268 Ly Thuong Kiet Street, Dien Hong Ward, Ho Chi Minh City, Viet Nam

<sup>2</sup>Vietnam National University Ho Chi Minh City, Linh Xuan Ward, Ho Chi Minh City, Viet Nam

\*Email: kieudotrungkien@hcmut.edu.vn

Received: 13 July 2023; Accepted for publication: 8 July 2024

**Abstract.** Silicon carbide (SiC) is a mineral with good technical properties and high economic value. However, the synthesis of SiC is expensive because it is carried out in high temperature environment (above 1500  $^{\circ}$ C). The synthesis of SiC from biomass can significantly reduce the synthesis temperature. One commonly used biomass material for synthesizing SiC is rice husk. However, the ability to synthesize SiC depends on the shape of the rice husk. The influence of rice husk morphology on the ability to synthesize SiC was investigated in this study. The experimental results showed that the original rice husk would give better SiC formation capacity than the rice husk powder. The amount of SiC formed using the original rice husk when impregnated with sodium silicate solution and pyrolyzed at 1200  $^{\circ}$ C is 18.3 % (wt.%), while it only reached 15.12 % (wt.%) with rice husk powder. The results of analysis of mineral composition, functional groups, and morphology by X-ray diffraction (XRD), Fourier transform infrared spectroscopy(FT-IR), and scanning electron microscopy (SEM) showed that the polymorphs of SiC are α-SiC and β-SiC. These minerals are the basis for the production of SiC from rice husks, which can be used as a wear-resistant material.

Keywords: silicon carbide, rice husk, pyrolysis, SiC/SiO<sub>2</sub>/C composite.

Classification numbers: 3.4.3, 2.9.4, 2.10.2.

## 1. INTRODUCTION

Silicon carbide is a mineral whose main components are silicon (Si) and carbon (C). It is a material with a chemical formula. Silicon carbide is a new material that is widely used in many fields thanks to its unique properties. SiC usually exists as small particles, thin sheets, or large plates. It is black in colour and has a hardness comparable to diamond. The SiC has a larger band gap than traditional silicon (Si) semiconductors. Therefore, the SiC is a very potential semiconductor material [1]. Due to its large band gap energy, it can withstand stronger electric fields, higher operating temperatures, and higher voltage surges than silicon. The SiC could become an ideal material for high power electronic applications. Silicon carbide is used to fabricate power electronic components such as motor control circuits, inverters, voltage stabilizers, and industrial electrical cabinets [2, 3]. Its high voltage and heat resistance help increase the efficiency and reduce the size of power electronic systems [4]. The SiC can be used

to fabricate blue, green, and white LEDs [5, 6]. The SiC LEDs have high brightness, long life, and energy saving compared to traditional LEDs [7]. In addition, the SiC is used in power conversion and control devices, including applications such as solar inverters, electric vehicles, and electrical systems on aircraft, ships, and hybrid vehicles [8, 9].

Besides potential applications in the fields of electricity and electronics, the SiC can also be applied as mechanical and heat-resistant materials thanks to its mechanical strength and high temperature resistance. The SiC has been used in the production of mechanical parts that require high hardness, high temperature resistance, and wear resistance [10, 11]. Applications include wear-resistant machinery parts, bearings, transmissions, and heat-resistant parts. The SiC has good heat resistance, so it is used in highly heat-resistant applications such as refractories, insulation materials, heat resistant pipes, and components in furnaces, boilers, and heating systems [12]. The SiC is used in the automotive industry to enhance critical components' hardness and wear resistance, such as brakes, bearings, valves, and pistons [13]. The SiC can also be used in applications to improve engine performance and reduce weight [14]. In addition to being the primary raw material, the SiC can also act as an additive to synthesize materials. SiC can be considered a foaming additive in ceramic products. When heating SiC in an  $O_2$  atmosphere, the SiC will form  $CO_2$  gas and contribute to the foaming of ceramic products [15]. Carbon produced during the decomposition of SiC can also be used as an additive in the production of  $Cr_2AlC$  [16], a potential compound in photocatalytic applications.

The above properties and applications show the role and potential of SiC materials. Currently, in industry, the SiC materials are usually made through a chemical reaction between compounds containing carbon (C) and silicon (Si). Commonly used materials for this synthesis are SiO<sub>2</sub> and C powder. With the traditional method, the SiC is usually formed at other high temperatures (above 1500 °C) [17]. Therefore, the synthesis of SiC is quite tricky, leading to high cost of this material. To solve this problem, many research groups have studied the preparation of SiC from biomass sources. The SiC can be synthesized from biomass materials at temperatures above 700 °C [18]. Creating SiC from biomass is also one of the methods that can be applied to treat agricultural wastes. M. Khangkhamano *et al.* have studied the fabrication of SiC from bagasse. Bagasse was pulverized and reacted with silicon at high temperatures. Their research results showed that SiC was formed at a temperature of 1800 °C [19]. The SiC can also be synthesized from sawdust. Using the same method, V. C. Bringas-Rodriguez *et al.* also obtained the SiC from sawdust at 500 °C [20]. In studies on the fabrication of SiC from biomass materials, rice husk is commonly used [18]. With the characteristic that rice husk contains a lot of silicon and carbon, this is a suitable source of raw material to create SiC.

However, few studies on rice husks have addressed the possibility of SiC formation when using rice husk materials with different morphologies. In this study, we fabricated SiC from crushed and original rice husks. By analytical methods such as chemical composition, X-ray diffraction, Fourier transform infrared spectroscopy, and scanning electron microscopy, the ability to form SiC was investigated. The results obtained provide information on the influence of rice husk morphology on the ability to synthesize SiC.

## 2. MATERIALS AND METHODS

Rice husk material (RH) was taken from Long An province, Viet Nam. The chemical composition of rice husks was determined by X-ray fluorescence and isotope ratio mass spectrometry methods. The chemical composition of RH is dominated by carbon (45.91 wt.%), silicon (8.38 wt.%), and hydrogen (6.12 wt.%), supplemented by several minor elements and a

substantial unquantified fraction (35.53 wt.%). Rice husks were washed and dried at 90 °C for 24 hours. After drying, the husks were divided into two groups. Group 1 (denoted as G1) was preserved with the original rice husk. Group 2 (denoted as G2) was milled in a crushing machine. The average particle size of group 2 is 47.71  $\mu$ m. Sodium silicate (Na<sub>2</sub>SiO<sub>3</sub>.nH<sub>2</sub>O - denoted as SS) was also used to add the silicon component. The density and module of sodium silicate are 1.5 g/mL and 2.9.

Two groups of RH were soaked in SS solution at a ratio of 5 g of rice husk/1 liter of SS for 24 hours. After that period of time, the SS would adhere to the surface of the rice husk. Thanks to that, the RH would be supplied with Si for the SiC generation reaction. The RH and SS mixtures were dried at different temperatures until the weight remained constant. After drying, the mixtures were sintered at 1200 °C in an oxygen-free atmosphere with a heating rate of 10 °C/min. Finally, the sintered samples were analyzed for properties such as formed SiC content, microstructure, and mineral composition to evaluate the reactivity to generate SiC of the two groups of materials.

The sintered powders were milled to a particle size of less than 150  $\mu$ m. Samples were taken according to ISO 5022 standards. The SiC content in the product was determined according to ISO 21068:2008 standards. The functional group was analyzed by Fourier transform infrared spectroscopy (FT-IR) with a scanning range of 450 - 4000 cm<sup>-1</sup> and a scanning step of 0.96425 cm<sup>-1</sup>. The mineral composition was determined by X-ray diffraction (XRD). Samples were measured at 2 $\theta$  from 5 to 70° with a scanning step of 0.019°. The microstructure was evaluated by scanning electron microscopy (SEM).

## 3. RESULTS AND DISCUSSION

RH is the source of Si and C for the SiC generation reaction. T. D. Dinh  $\it et al.$  have shown that RH can be a source of raw materials to provide SiO<sub>2</sub> [21]. However, the Si content in RH is low. It is necessary to add materials to provide Si components. Figure 1 shows the results of determining the adhesion ability of SS on the RH surface of two groups of RH particles at different drying temperatures.

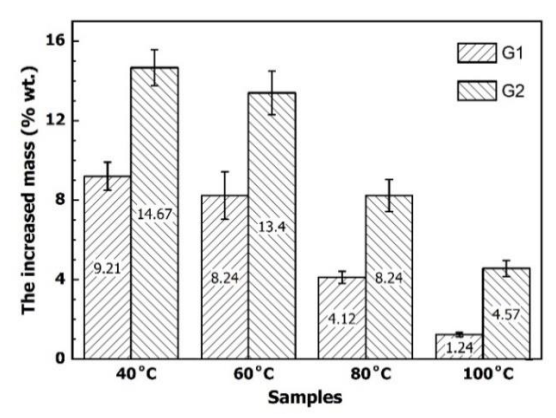


Figure 1. Mass increase of RH material groups after soaking (% wt.).

The results in Figure 1 also show a significant mass difference between the G1 and G2 groups. Considering the same drying temperature, the G1 sample with a large particle size gained less mass than the G2 sample. The results show that particle size affects the ability to retain SS. The smaller the particle size of the material, the greater the ability to keep SS. In this case, the ability to keep SS is related to the surface area of the material. Observing

the SEM images in Figure 2, the G2 sample has a grain size many times smaller than the G1 sample. If the material has a small particle size, the surface area of the material will increase. As the area exposed to SS increases, the ability to retain SS also increases. The ability to hold SS also contributes to an increase in the amount of Si for the G2 sample. Therefore, the G2 sample is expected to form a lot of SiC after calcination. When comparing different drying temperatures, the results in Figure 1 show that the higher the drying temperature, the lower the amount of SS kept. As the drying temperature increases, the drying speed will also increase. The SS components will be swept away by water evaporation. Therefore, the amount of SS retained in the RH decreases.

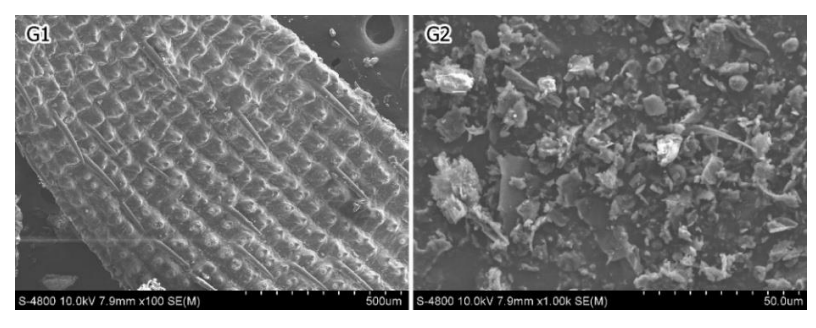


Figure 2. SEM images of RH of group 1 (G1) and group 2 (G2).

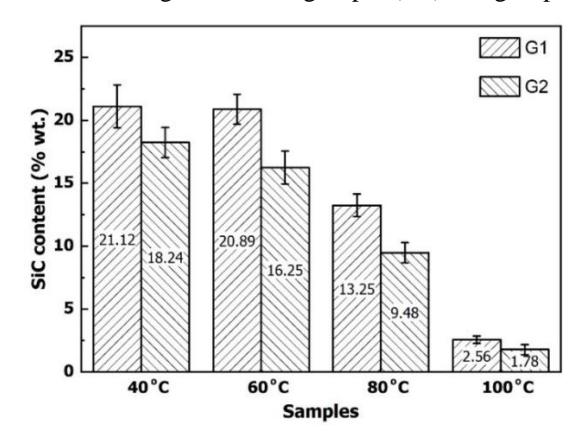


Figure 3. SiC content of samples G1 and G2 after sintering at 1200 °C (wt.%).

The G1 and G2 samples, after being impregnated with SS and dried at different temperatures (40, 60, 80, and 100 °C), were sintered at 1200 °C to synthesize SiC. The sintered G1 and G2 samples were analyzed to determine the amount of SiC formed. Figure 3 presents the results of determining SiC content according to ISO 21068:2008 standards. The results in Figure 3 show that SiC was synthesized when the samples were sintered at 1200 °C. Figure 3 also shows that the SiC content decreases with increasing drying temperature, indicating the role of SS in the process of SiC generation. As the drying temperature increased, the amount of SS kept on the RH surface decreased. The Si composition in the system is also reduced, so the amount of SiC formed during the heating process also decreases. Considering the two groups of particles, the results in Figure 3 are in contrast to those in Figure 1. The G1 group materials showed higher SiC content than the G2 group in all samples. Some previous studies have demonstrated that the SiC generation reaction is reduced when the CO<sub>x</sub> content in the system increases [22, 23]. The mechanism of SiC formation is shown in chemical equations from (1) to (5). So, the SiC content will also decrease. In this case, the space between the particles increases because the G1 group

has a larger particle size than the G2 group. The  $CO_x$  formed during the pyrolysis of RH is quickly released. Since then, the  $CO_x$  content in the system also decreases, allowing more SiC to be produced.

Figure 1 and Figure 3 show that the G1 sample with high ventilation gives a higher SiC content than the G2 sample under the same synthesis conditions. In addition, 40 °C and 60 °C are suitable temperatures for drying SS and RH. However, 40 °C will give more drying time than 60 °C. Therefore, 60 °C is chosen for drying SS and RH. The G1 and G2 group samples sintered at 1200 °C will be analyzed by FT-IR and XRD to determine the mineral composition. Figure 4 show the results of FT-IR analysis and XRD patterns.

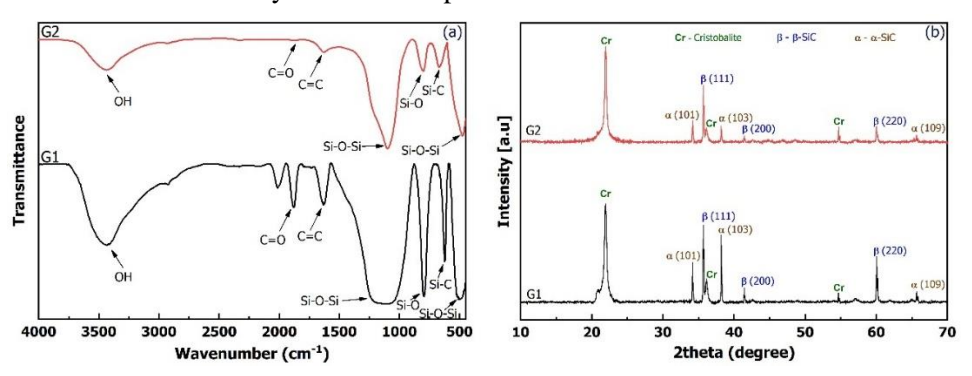


Figure 4. FT-IR spectra (a) and XRD patterns (b) of samples G1 and G2 after sintering at 1200 °C.

The FT-IR results in Figure 4 are typical for SiC products synthesized from biomass sources. The vibration at 3100 - 3600 cm<sup>-1</sup> on the FT-IR spectrum is characteristic of the O-H group [24]. The O-H group represents the moisture in the samples and the vibration characteristic of the Si-C covalent bond is found at position 789 cm<sup>-1</sup> [24]. In addition, because the precursor is a biomass source, the product will contain C=O and C=C groups at the wavenumber positions of 1720 and 1632 cm<sup>-1</sup> [25]. The vibrations of the Si-O and Si-O-Si bonds at 1059, 812, and 464 cm<sup>-1</sup> [24, 26] are typical for the Si component that does not react entirely and is oxidized to SiO<sub>2</sub> afterwards. From the FT-IR results, there was SiC formation at 1200 °C in both G1 and G2 groups. However, the formed SiC contains many impurities. Impurities formed after sintering are typical by-products of SiC synthesis from biomass sources [27]. The SiC made from biomass sources can be used in applications with low SiC purity. If some chemical and thermal methods remove other components, such as C and SiO<sub>2</sub>, pure SiC can be completely formed from rice husks.

The XRD method was also used to determine the mineral composition of the G1 and G2 groups after sintering (Figure 4b). The XRD patterns of the samples after sintering show similarities in mineral composition. The XRD results also confirmed the mineral composition of the product as indicated in the FTIR spectra. For the G1 and G2 samples, minerals, including cristobalite (SiO<sub>2</sub>),  $\alpha$ -SiC, and  $\beta$ -SiC, were formed after sintering. The mineral cristobalite (JCPDS card No. 39-1425) is represented at diffraction positions of 21.99°, 36.5°, and 54.2° [28]. Cristobalite is the high-temperature polymorph of SiO<sub>2</sub>. It is formed by heating SiO<sub>2</sub> without a catalyst [29]. Mineral  $\beta$ -SiC (JCPDS card No. 29-1129) is present at diffraction positions of 35.6°, 41.6°, and 60° [24].  $\beta$ -SiC is the low-temperature polymorph of SiC. This is a common mineral found in low-temperature SiC synthesis. It is also a transition mineral before the formation of  $\alpha$ -SiC. The  $\alpha$ -SiC mineral (JCPDS card No. 01-073-1664) is represented at diffraction positions of 34.1°, 38°, and 66.5° [24].  $\alpha$ -SiC is the high-temperature polymorph of SiC. Previous studies have shown that  $\alpha$ -SiC usually forms at sintering temperatures above 1500

°C. This result indicates that it is possible to create different SiC polymorphs at low temperatures by sintering RH impregnated with SS.

In addition to forming similar minerals in the G1 and G2 groups, the XRD patterns of the two samples also show the difference in the intensity of the peaks related to SiC minerals. This difference is easily observed when comparing the intensity ratio of the SiC peaks to the cristobalite peaks. The results show that the intensity of SiC peaks in the G1 sample is higher than in the G2 sample. It proves that SiC crystals in the G1 sample grow better than in the G2 sample. This observation again proves that the formation of SiC minerals in the G1 sample is more favorable than that in the G2 sample. The reason for this advantage is that the ventilated form of the G1 model allows  $CO_x$  to escape quickly.

### 4. CONCLUSIONS

In this study, SiC was made from RH impregnated with SS and sintered at 1200  $^{\circ}$ C. The analysis results of SS keeping capacity, chemical composition, functional groups, and mineral composition also showed the ability to create SiC of two groups of raw materials, original RH (G1 group) and crushed RH (G2 group). The G2 group with small particle size and large surface area will have better SS retention ability during RH impregnation with SS. However, the G1 group with good ventilation will help the  $CO_x$  formed during pyrolysis to release quickly. As a result, the balance of the chemical equation for the formation of SiC will shift from left to right. The content of formed SiC of the G1 sample is larger than that of the G2 sample. The formed SiC has two polymorphs, including  $\beta$ -SiC and  $\alpha$ -SiC. They are two low- and high-temperature polymorphs of SiC. In addition, there is also the presence of cristobalite (SiO<sub>2</sub>) and carbon in the composition of the samples after sintering. They are products that form when the C and Si precursors react uncompletely. Therefore, SiC synthesized from biomass can be used in applications without high purity. This can also be a precursor to forming pure SiC through C and SiO<sub>2</sub> reduction processes.

*Acknowledgements.* This research is funded by Vietnam National University Ho Chi Minh City (VNU-HCM) under grant number: B2023-20-18. We acknowledge Ho Chi Minh City University of Technology (HCMUT), VNU-HCM for supporting this study.

*CRediT authorship contribution statement.* Kieu Do Trung Kien: Methodology, Funding acquisition. Ong Dieu Hanh: Formal analysis. Nguyen Hoang Thien Khoi: Formal analysis. Huynh Ngoc Minh: Investigation, Supervision.

**Declaration of competing interest.** The authors declare that they have no known competing financial interests or personal relationships that could have appeared to influence the work reported in this paper.

#### **REFERENCES**

- 1. Neudeck P. G. Progress in silicon carbide semiconductor electronics technology, J. Electron. Mater. **24** (1995) 283-288. https://doi.org/10.1007/BF02659688
- 2. Kong X., Nie R., and Yuan J. Shape stabilized three-dimensional porous SiC-based phase change materials for thermal management of electronic components, Chem. Eng. J. **462** (2023) 142168. https://doi.org/10.1016/j.cej.2023.142168
- 3. Singh S., Chaudhary T., and Khanna G. Recent advancements in wide band semiconductors (SiC and GaN) technology for future devices, Silicon **14** (11) (2022) 5793-5800, 2022. https://doi.org/10.1007/s12633-021-01362-3

- 4. Alves L. F. S, Gomes R. C. M., Lefranc P., Pegado R. D. A., Jeannin P. O. Luciano B. A., and Rocha F. V. SIC power devices in power electronics: An overview, Brazilian Power Electronics Conference (COBEP), Barzil, 2017, pp. 1-8. https://doi.org/10.1109/COBEP.2017.8257396
- 5. Edmond J. A., Kong H. S., and Carter Jr C. H. Blue LEDs, UV photodiodes and high-temperature rectifiers in 6H-SiC, Phys. B (Amsterdam, Neth.) **185** (1-4) (1993) 453-460. https://doi.org/10.1016/0921-4526(93)90277-D
- 6. Feng D. H., Jia T. Q., Li X. X., Xu Z. Z., Chen J., Deng S. Z., Wu Z. S., and Xu N. S. Catalytic synthesis and photoluminescence of needle-shaped 3C–SiC nanowires, Solid State Commun. **128** (8) (2003) 295-297. https://doi.org/10.1016/j.ssc.2003.08.025
- J. Edmond J., Abare A., Berman M., Bharathan J., Bunker K. L., Emerson D., Haberern K., Ibbetson J., Leung M., Russel P., and Slater D. High efficiency GaN-based LEDs and lasers on SiC, J. Cryst. Growth 272 (1-4) (2004) 242-250. https://doi.org/10.1016/j.jcrysgro.2004.08.056
- 8. Ni Z., Lyu X., Yadav O. P., Singh B. N., Zheng S., and Cao D. Overview of real-time lifetime prediction and extension for SiC power converters, IEEE T. Power Electr. **35** (8) (2019) 7765-7794. https://doi.org/10.1109/TPEL.2019.2962503
- Louro P., Vieira M., Fernandes M., Costa J., Vieira M. A., Caeiro J., Neves N., and Barata M. Optical demultiplexer based on an a-SiC: H voltage controlled device, Phys. Status Solidi C 7 (3-4) (2010) 1188-1191. https://doi.org/10.1002/pssc.200982702
- 10. Prasad K. E. and Ramesh K. Hardness and mechanical anisotropy of hexagonal SiC single crystal polytypes, J. Alloys Compd. **770** (2019) 158-165. https://doi.org/10.1016/j.jallcom.2018.08.102
- 11. Su L., Wang H., Niu M., Fan X., Ma M., Shi Z., and GUo S. W. Ultralight, recoverable, and high-temperature-resistant SiC nanowire aerogel, ACS nano **12** (4) (2018) 3103-3111. https://doi.org/10.1021/acsnano.7b08577
- 12. Wang H. F., Bi Y. B., Zhou N. S., and Zhang H. J. Preparation and strength of SiC refractories within situ  $\beta$ -SiC whiskers as bonding phase, Ceram. Int. **42** (1) (2016) 727-733. https://doi.org/10.1016/j.ceramint.2015.08.172
- 13. Borrero-López O., Ortiz A. L., Guiberteau F., and Padture N. P. Microstructural design of sliding-wear-resistant liquid-phase-sintered SiC: an overview, J. Eur. Ceram. Soc. 27 (11) (2007) 3351-3357. https://doi.org/10.1016/j.jeurceramsoc.2007.02.190
- 14. Spitsberg I. and Steibel J. Thermal and environmental barrier coatings for SiC/SiC CMCs in aircraft engine applications, Int. J. Appl. Ceram. Technol. **1** (4) (2004) 291-301. https://doi.org/10.1111/j.1744-7402.2004.tb00181.x
- 15. Kien K. D. T., Thuy D. D. X., Nhi N. V. U., and Minh D. Q. The formation of red copper Glaze in an Oxidizing Atmosphere, Iran. J. Mater. Sci. Eng. **20** (3) (2023) 1-9. https://doi.org/10.22068/ijmse.3141
- 16. Ta Q. T. H., Tran, N. M., and Noh J. S. Pressureless manufacturing of  $Cr_2AlC$  compound and the temperature effect, Mater. Manuf. Processes **36** (2) (2021) 200-208. https://doi.org/10.1080/10426914.2020.1819547
- 17. Krishnarao R., Godkhindi M., Chakraborty M., and Mukunda P. Formation of SiC whiskers from compacts of raw rice husks, J. Mater. Sci. **29** (1994) 2741-2744. https://doi.org/10.1007/BF00356826

- 18. Khai T. V., Minh H. N., Nhi N. V. U., and Kien K. D. T. Effect of composition on the ability to form SiC/SiO<sub>2</sub>-C composite from rice husk and silica gel, J. Ceram. Process. Res. **22** (2) (2021) 246-251. https://doi.org/10.36410/jcpr.2021.22.2.246
- 19. Khangkhamano M., Singsarothai S., Kokoo R., and Niyomwas S. Conversion of bagasse ash waste to nanosized SiC powder, Int. J. Self-Propag. High-Temp. Synth. **27** (2018) 98-102. https://doi.org/10.3103/S1061386218020103
- 20. Bringas-Rodríguez V., Huamán-Mamani F., Paredes-Paz J., and Gamarra-Delgado J. Evaluation of thermomechanical behavior in controlled atmospheres of silicon carbide obtained from sawdust residues of the Peruvian timber industry, Mater. Today: Proc. **33** (2020) 1835-1839. https://doi.org/10.1016/j.matpr.2020.05.175
- 21. Dinh T. D., Nguyen Q. L., Vu M. D., Tran T. M. H., Tran T. H. N, Nguyen M. H., and Pham T. D. Adsorption characteristics of Cu2+ on CeO2/SiO2 nanomaterials based on rice husk and its application to pre-concentration and determination in food samples, Colloid Polym. Sci. (2023). https://doi.org/10.1007/s00396-023-05140-y
- 22. Wang Y., Zhang L., Zhang X., Zhang Z., Tong Y., Li F., Wu J. C. S., and Wang X. Openmouthed β-SiC hollow-sphere with highly photocatalytic activity for reduction of CO<sub>2</sub> with H<sub>2</sub>O, Appl. Catal. B **206** (2017) 158-167. https://doi.org/10.1016/j.apcatb.2017.01.028
- 23. Goto T. and Homma H. High-temperature active/passive oxidation and bubble formation of CVD SiC in O<sub>2</sub> and CO<sub>2</sub> atmospheres, J. Eur. Ceram. Soc. **22** (14-15) (2022) 2749-2756. https://doi.org/10.1016/S0955-2219(02)00139-5
- 24. King S., French M., Bielefeld J., and Lanford W. Fourier transform infrared spectroscopy investigation of chemical bonding in low-k a-SiC: H thin films, J. Non-Cryst. Solids **357** (15) (2011) 2970-2983. https://doi.org/10.1016/j.jnoncrysol.2011.04.001
- 25. Kien K. D. T., Tuan P. D., Okabe T., Minh D. Q., and Khai T. V. Study on sintering process of woodceramics from the cashew nutshell waste, J. Ceram. Process. Res. **19** (6) (2018) 472-478.
- 26. Kien K. D. T., Minh D. Q., Minh H. N., and Nhi N. V. U. Synthesis of TiO<sub>2</sub>-SiO<sub>2</sub> from tetra-n-butyl orthotitanate and tetraethyl orthosilicate by the sol-gel method applied as a coating on the surface of ceramics, Ceramics–Silikáty **67** (1) (2023) 58-63. https://doi.org/10.13168/cs.2023.0002
- 27. Chiew Y. L. and Cheong K. Y. A review on the synthesis of SiC from plant-based biomasses, Mater. Sci. Eng. B **176** (13) (2011) 951-964. https://doi.org/10.1016/j.mseb.2011.05.037
- 28. Fneich H., Vermillac M., Neuville D. R., Blanc W., and Mehdi A. Highlighting of LaF3 reactivity with  $SiO_2$  and  $GeO_2$  at high temperature, Ceramics 5 (2) (2022) 182-200. https://doi.org/10.3390/ceramics5020016
- 29. Taylor N. W. and Lin C. Y. Effect of various catalysts on conversion of quartz to cristobalite and tridymite at high temperatures, J. Am. Ceram. Soc. **24** (2) (1941) 57-63. https://doi.org/10.1111/j.1151-2916.1941.tb14821.x